Bull. Mater. Sci., Vol. 26, No. 1, January 2003, pp. 199–205. © Indian Academy of Sciences.

Effect of alloying on the electronic structure and magnetic properties of Fe, Co and Ni with Au and Ag

ASHISH BHATTACHARJEE, MESBAHUDDIN AHMED*, ABHIJIT MOOKERJEE[†] and AMAL HALDER[#]

Department of Physics, [#]Department of Mathematics, University of Dhaka, Dhaka 100, Bangladesh
[†]S. N. Bose National Centre for Basic Sciences, JD Block, Sector 3, Salt Lake City, Kolkata 700 098, India

Abstract. We use the self-consistent, augmented space recursion technique to study the electronic structure and magnetic properties of alloys of the transition metals, Fe, Co and Ni with the noble metals, Ag and Au. We analyse the effect of local environment and the hybridization between the constituent bands on the electronic and magnetic properties.

Keywords. Magnetism; alloys.

1. Introduction

Recently there have been several studies on the magnetism of thin overlayers of transition metals like Fe on noble metal substrates (Blügel 1997; Mookerjee *et al* 2000). It was noted that the magnetic moment on a surface 'magnetic' atom depended sensitively on both the local environment of the atom, as well as hybridization of its *d*-bands with the substrate. Looser binding at the surface narrows the *d*-bands, whereas hybridization had an effect of increasing the band width. Consequently, according to the Stoner criterion, the former enhances magnetic moment while the latter deceases it. The final result is a subtle interplay between these competing effects. The aim of this communication is to study whether a similar effect occurs on alloying. The two constituent atoms are intermixed and their local environment plays the crucial role.

It has been known experimentally that diluting Fe with Au, eventually leads to the destruction of the averaged magnetic moment around 14 atomic % of Au, although the local moment of Fe atoms themselves may not be zero. To study the comparative effect of hybridization we have chosen to alloy the transition metals, Fe, Co and Ni with the noble metals, Au and Ag. After examining the band structures of the face-centred structures of these metals, the extension of the *s–d* hybridized bands are shown in table 1.

We note that the *d*-bands of the three transition metals are quite well separated from those of Ag and Au. The other fact known is that the local magnetism of Co and Ni is much weaker than that of Fe. In particular that of Ni is fragile and depends strongly on how many Ni atoms are in the vicinity of the atom under consideration. The aim of this work is to study how the local and averaged magnetization changes as we form these alloys at different constituent concentrations.

We shall consider hybridized *s* and *d* electrons in these metals as contributing to a Fermi liquid ground state. We shall study the charge and spin densities using the local spin density approximation (LSDA) in the tight-binding linearized muffin–tin orbital basis (TB–LMTO), introduced by Andersen and Jepsen (1984). The disorder effect is studied using the augmented space recursion (ASR) introduced by us earlier (Saha *et al* 1994).

2. Methodology

2.1 *The magnetic phases*

Description of different magnetic phases within the LSDA involves the evolution of local magnetic moments in the vicinity of ion cores because of the distribution of the valence electron charge. Each lattice site in the face centred cubic structure is occupied by an ion core: in our case randomly by either Fe or Au. Associated with each ion core is a cell or a sphere, so defined that the charge density contained in the sphere is thought to belong to that ion core along. Ideally such cells or spheres should

Table 1. Approximate location and width of the *s–d* hybridized bands of Au, Ag, Cu and Fe, Co, Ni.

Noble metal	Width of *s–d* bands (Ryd)
Au	$-0{\cdot}75 < E < -0{\cdot}4$
Ag	$-0{\cdot}65 < E < -0{\cdot}35$
Transition metal	**Width of *s–d* bands (Ryd)**
Fe	$-0{\cdot}4 < E < 0{\cdot}15$
Co	$-0{\cdot}35 < E < 0{\cdot}10$
Ni	$-0{\cdot}3 < E < 0{\cdot}05$

*Author for correspondence

not overlap and this division of space is to a certain extent arbitrary. Within these cells the valence electrons carrying spine σ sees a binary random spin-dependent potential, $V_s^l(r)$, where l = X or Fe, where X is either Ag or Au and $s = \uparrow$ or $\downarrow$.

The charge density within the cells can be obtained from solving the Schrödinger equation within the LSDA. The charge density over the solid can be written as

$$\rho_s(r) = -(1/\pi)\Im m \sum_L \int_{-\infty} E_F [x\langle G^{Fe,s}(r,r,E)\rangle_{av} + (1-x)\langle G^{Au,s}(r,r,E)\rangle_{av}]\, dE, \quad (1)$$

where, $\langle G^{X,s}_{LL}(r,r,E)\rangle_{av}$ is the component projected Green functions with the site r occupied by an X type ion-core potential corresponding to spin s. The X sites are almost spin independent (except for a very small induced moment) if X is a noble metal, but carries a local magnetic moment if X is one of the transition metals.

For the random ferromagnetic phase we proceed as follows: we consider all cells to be statistically identical in that they all carry identical average charge densities. We shall borrow the notation $\sim$ of Andersen and Jepsen (1984) to write functions like $\tilde{f}(r_R)$ which are as long as r lies in a cell labelled by R and is zero outside $(r_R = r - R)$. The ferromagnetic charge densities are defined as

$$\rho_1(r) = \sum_R \tilde{\rho}_\uparrow(r_R),$$

$$\rho_2(r) = \sum_R \tilde{\rho}_\downarrow(r_R). \quad (2)$$

The magnetic moment per cell (atom) is then defined by

$$m = (1/N)\int d^3r[\rho_1(r) - \rho_2(r)]$$

$$= (1/N)\sum_R \int_{r\le S} d^3r[\tilde{\rho}_\uparrow(r_R) - \tilde{\rho}_\downarrow(r_R)]$$

$$= (1/N)\sum_R \int_{r\le S} d^3r m_R(r_R).$$

Since all cells are statistically identical, the above calculation need be done only in one typical cell. Within the TB–LMTO–ASA the cells are replaced by inflated atomic spheres and the remaining interstitial is neglected. The problem is then one of a binary alloy with an almost non-magnetic charge density due to the noble metal ion cores and a magnetic one due to the transition metal ones.

For the paramagnetic case, the charge densities become independent of spin: $\rho_1(r) = \rho_2(r)$. The local moment density itself vanishes. Not only is the global magnetic moment per cell (atom) zero, but so is the magnetic moment in any cell. This distinguishes the paramagnetic phase from the antiferromagnetic one.

In both the above cases the problem reduces to that of a binary random alloy between non magnetic X atoms and moment carrying (or non-magnetic in the case of paramagnetic) Fe atoms. It is important to note here that the description is basically from an itinerant viewpoint. The valence electron cloud which gives rise to the local moments because of a persistent difference between the up and down charge densities in the ion-core cells, is truly delocalized and does not belong to any particular ion-core.

2.2 *The augmented space recursion*

In an earlier communication we have described how to deal with binary (Dasgupta *et al* 1993) and ternary alloys (Saha and Mookerjee 1997) within the framework of the tight-binding linearized muffin–tin orbitals method (TB–LMTO) of Andersen and Jepsen (1984). This provides us with a first principles determination of the configuration averaged Green function of the disordered alloy. Subsequently we may obtain the density of states, the Fermi energies, the charge densities and total energies of the system. We start from the most-localized tight binding Hamiltonian derived systematically from the local spin density approximation (LSDA)

$$H = \sum_{RL} C_{RL}\hat{\hat{N}}_R \otimes \hat{\hat{N}}_L + \sum_{RL}\sum_{R'L'} \Delta^{1/2}_{RL} S^b_{RL,R'L'} \Delta^{1/2}_{R'L'} T_{R,R'} \otimes T_{L,L'}, \quad (3)$$

where, C_{RL} and Δ_{RL} randomly take the values corresponding to the constituents A and B with probabilities, x_A and x_B, unless $R = R_0$, the site at which the component projected Green functions are to be calculated. Here they take the specific values corresponding to either the A or the B constituent.

Let us write the expression for the partial Green function where the site, R_0, is occupied by a l type of atom. We shall, for the sake of brevity drop the indices R and L, for the time being.

$$G^l_{R_0L,R_0L} = \langle R_0L\,|\,(E - C - \Delta^{1/2} S \Delta^{1/2})^{-1}\,|\,R_0L\rangle$$

$$= \left\langle R_0L \left| \Delta^{-1/2}\left(\frac{E-C}{\Delta} - S\right)^{-1}\Delta^{-1/2}\right| R_0L\right\rangle$$

$$= \left\langle R_0L \left| \left(\Delta_l \frac{E-C}{\Delta} - \Delta_l^{1/2} S \Delta_l^{1/2}\right)^{-1}\right| R_0L\right\rangle.$$

Writing out in full, we get an expression for $G^l_{R_0L,R_0L}$ as

$$\left\langle R_0 L \left| \left(\sum_{RL} \boldsymbol{x}_{RL}(E) \hat{\hat{N}}_R \otimes \hat{\hat{N}}_L \right. \right. \right.$$

$$\left. \left. \left. - \sum_{RL} \sum_{R'L'} \Delta^{1/2}_{l,RL} S_{RL,R'L'} \Delta^{1/2}_{l,RL} \hat{O}_{RR'} \otimes \hat{O}_{LL'} \right)^{-1} \right| R_0 L_0 \right\rangle.$$

The only random parameters here are $\boldsymbol{x}_{RL}$ (E). If $R = R_0$, $\boldsymbol{x}_{R_0,L}(E) = E - C^{l}_{R_0 L}$, while if $R \neq R_0$ then we may write the random potential parameter as follows

$$x_{RL} = x^{B}_{L} + (x^{A}_{L} - x^{B}_{L}) n_R.$$

The occupation variables $\{n_R\}$ randomly take the values 1, 0 according to whether the site labelled by R is occupied by the constituents A, or B. In a perfectly random alloy the probability of such occupations are proportional to the concentrations of the constituents: x_A and x_B.

$$p(n_R) = x_A \boldsymbol{d}(n_R - 1) + x_B \boldsymbol{d}(n_R),$$

which can be rewritten as a continued fraction as

$$p(n_r) = (-1/\boldsymbol{p}) \Im m \frac{1}{n^{+}_{R} - x_B - \dfrac{x_A x_B}{n^{+}_{R} - x_A}}.$$

The augmented space theorem [1] now constructs operators $M^{(R)}$ corresponding to the variables, n_R, in the configuration space of rank 2^N.

$$M^{(R)} = \begin{pmatrix} x_B & \sqrt{x_A x_B} \\ \sqrt{x_A x_B} & x_A \end{pmatrix}. \tag{4}$$

Application of the augmented space theorem first constructs a configuration space, Φ, spanned by all $2^{(N-1)}$ configurations at all sites except R_0. Each site has two configurations labelled by 1 and 2. The null configuration $|\{\boldsymbol{ø}\}|\{\boldsymbol{f}\}\rangle$ is the configuration {111111111…….}. The component projected Green function is then given by

$$\langle G^{l}_{R_0 L_0, R_0 L_0} \rangle_{\text{av}} = \langle R_0 L_0 \{\boldsymbol{f}\} | (E - C^{l}_{L}) P_{R_0} \otimes P_{L_0} \otimes I + \ldots$$

$$\cdots + \left\{ \sum_{R \neq R_0, L} \langle\langle \boldsymbol{x}_L(E) \rangle\rangle P_R \otimes P_L \otimes I + \ldots \right.$$

$$\cdots + x^{(2)}_{L}(E) P_R \otimes P_L \otimes P^{R}_{2} + + x^{(3)}_{L}(E) P_R \otimes P_L \otimes T^{R}_{12} \} - \cdots$$

$$\left. \cdots - \sum_{RL} \sum_{R'L'} \Delta^{l\,1/2}_{L} S_{RL,R'L'} \Delta^{l\,1/2}_{L'} T_{RR'} \otimes T_{LL'} \otimes I)^{-1} | R_0 L_0 \{\boldsymbol{f}\} \right\rangle . \tag{5}$$

The five different types of potential parameters in augmented space: $C^{l}_{L}, \Delta^{l\,1/2}_{L}$, $\langle\langle \boldsymbol{x}_L(E) \rangle\rangle$, $x^{(2)}_{L}(E)$ and $x^{(3)}_{L}(E)$ are obtained from the TB–LMTO–ASR and (4).

$$x^{(2)}_{L}(E) = (x_B - x_A)(x_A(E) - x_B(E)),$$

$$\boldsymbol{x}^{(3)}_{L}(E) = \sqrt{x_B x_A}\,(\boldsymbol{x}_A(E) - \boldsymbol{x}_B(E)).$$

Note that the potential parameters are energy dependent. We, therefore, carry out the seed recursion proposed by Ghosh *et al* (1999) to obtain the required component projected Green functions, from them the electronic structure and local magnetic moments in the alloys.

2.3 *Computational details*

For the calculation of the component projected averaged density of states of the binary model related to the ferromagnetic and paramagnetic we have used a real space cluster of 400 atoms and an augmented space shell up to the sixth nearest neighbour from the starting state. Eight pairs of recursion coefficients were determined exactly and the continued fraction terminated by the analytic terminator due to Luchini and Nex. In a recent paper, Ghosh *et al* (1997) have shown the convergence of the related integrated quantities, like the Fermi energy, the band energy, the magnetic moments and the charge densities, within the augmented space recursion. The convergence tests suggested by the authors were carried out to prescribed accuracies. We have reduced the computational burden of the recursion in the full augmented space by using the local symmetries of the augmented space to reduce the effective rank of the invariant subspace in which the recursion is confined (Dasgupta *et al* 1996) and using the seed recursion methodology (Ghosh *et al* 1999) with fifteen energy seed points uniformly across the spectrum. Both the reduction techniques have been described in detail in the referenced papers and the readers are referred to them for details. It is important to emphasize this point, since there has been erroneous statements made earlier that although the augmented space recursion method is attractive mathematically, it is not feasible for application as a computational technique is realistic alloys. Further, it has been shown (Dasgupta *et al* 1996) that augmented space recursion with an analytic terminator always produces herglotz results, whether we use the homogeneous disorder model as in this paper or the version including short-ranged order (Mookerjee and Prasad 1993; Dasgupta *et al* 1993) or local lattice distortions (Saha *et al* 1996).

We have chosen the Wigner–Seitz radii of the two constituent atoms, Fe and Au, in such a way that the average volume occupied by the atoms is conserved. Within this constraint we have varied the radii so that the final configuration has neutral spheres. This eliminates the necessity to include the averaged Madelung energy part in the total energy of the alloy. The definition and computation of the Madelung energy in a random alloy had faced controversy in recent literature (Gonis *et al*

1996) and to this date no satisfactory resolution of the problem exists. Simultaneously we have made sure that the sphere overlap remains within the 15% limit prescribed by Andersen.

The calculations have been made self-consistent in the LSDA sense, i.e. at each stage the averaged charge densities are calculated from the augmented space recursion and the new potential is generated by the usual LSDA techniques. This self-consistency cycle was converged in both total energy and charge to errors of the order 10^{-5}. We have also minimized the total energy with respect to the lattice constant. The quoted results are those for the minimum configuration. No short ranged order due to chemical clustering has been taken into account in these calculations, nor any lattice distortions due to the size differences between the two constituents.

3. Results

Figures 1 (a)–(c) show the component density of states for AuFe, AuCo and AuNi as functions of concentrations of the constituents. The first thing to note is that in all cases the *s–d* bands of Au and those of Fe, Co and Ni do not overlap much. Hybridization effects are not large and all three are examples of split band alloys. Consequently in the low concentration regimes of either Au or Fe, Co and Ni we have impurity-like peaks of the dilute constituent.

For AuFe, the Au projected density of states are hardly exchange split and straddle the energy range around −0·6 to −0·5 Ryd. It starts as an impurity-like sharp peak for the 10% of Au alloy and broadens to a wide Au *s–d* band at 80% of Au alloy. As the concentration of Fe increases the up-spin band almost remains fixed around −0·3 Ryd, the down-spin band shifts upwards in energy, starting from the Fermi energy at −0·15 Ryd for the Fe 10% alloy crossing it to 0·0 Ryd for the Fe 80% alloy.

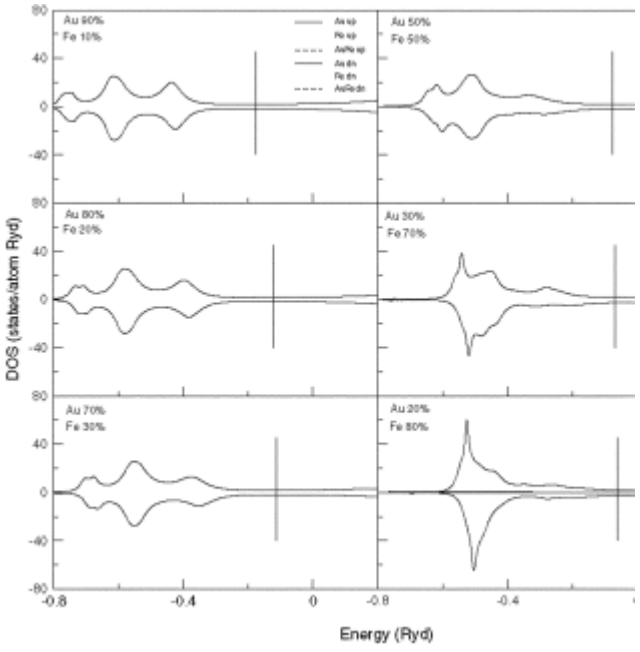

Figure 1a. Component density of states for AuFe for different concentrations.

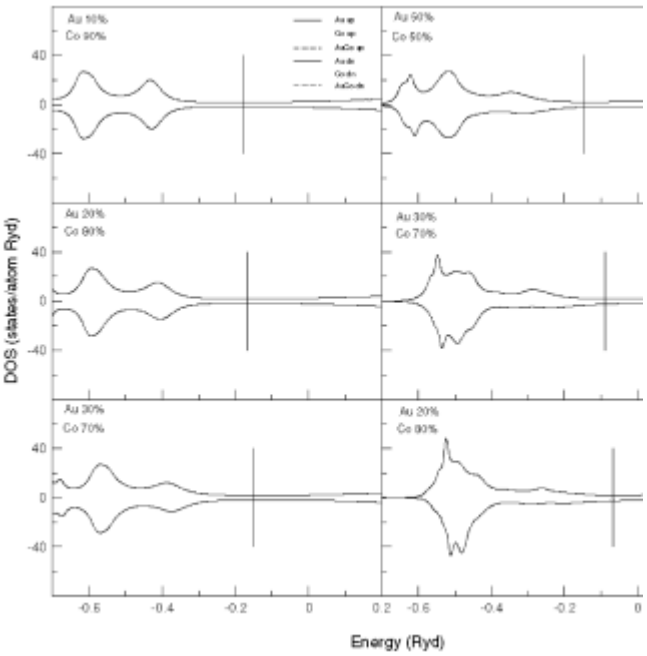

Figure 1b. Component density of states for AuCo for different concentrations.

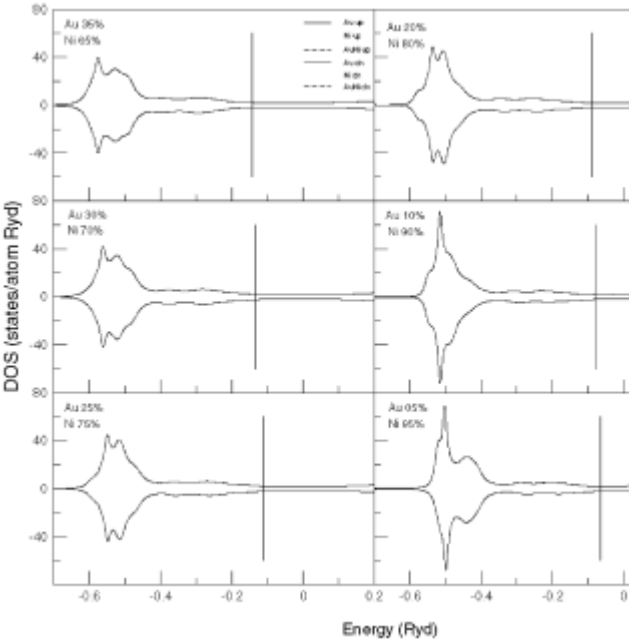

Figure 1c. Component density of states for AuNi for different concentrations.

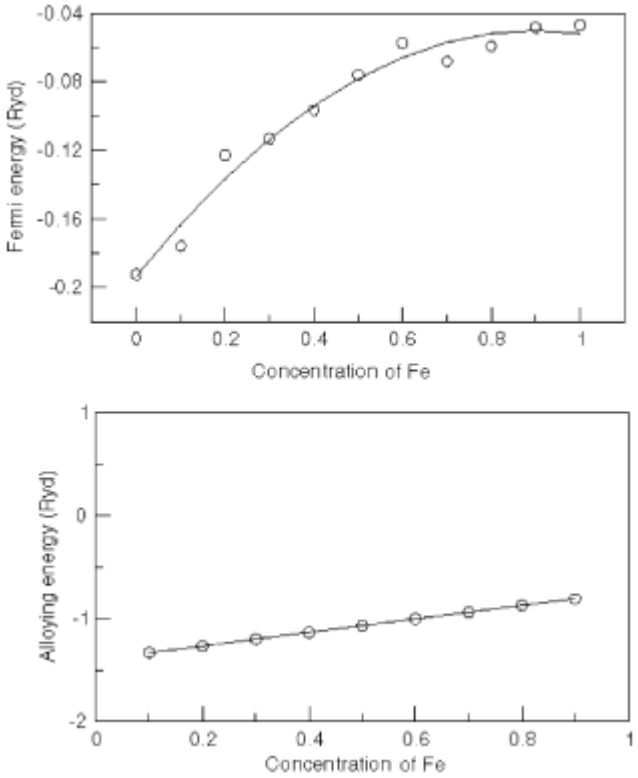

Figure 2a. Fermi and alloying energies for AuFe for different concentrations.

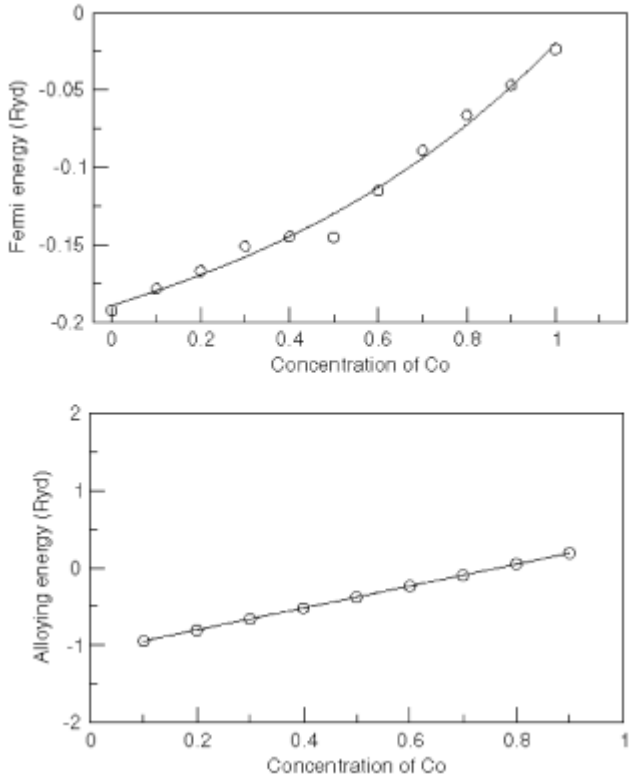

Figure 2b. Fermi and alloying energies for AuCo for different concentrations.

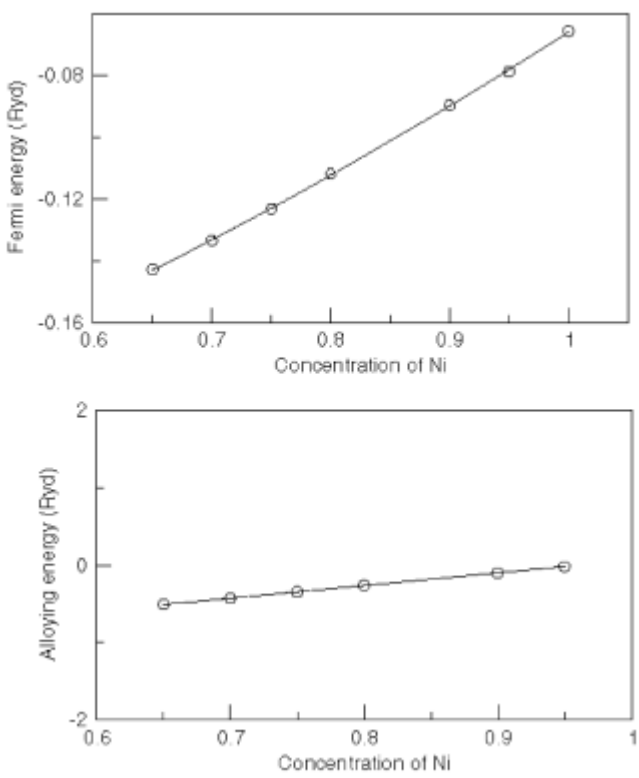

Figure 2c. Fermi and alloying energies for AuNi for different concentrations.

Figure 2(a) shows the behaviour of the Fermi energy and alloying energy as functions of the Fe concentation in AuFe. The exact behaviour of the Fermi energy depends sensitively on the exact shapes of the density of states and band filling. Since the Fe bands lie higher in energy than Au, increasing Fe concentration leads to upward shift in the Fermi energy. A similar shift is observed for the alloying energy, indicating increasing alloy stability with increasing Fe concentration.

Figure 3(a) shows the behaviour of the local magnetic moments on Fe and Au as well as the total magnetic moment of the alloy (per atom) as functions of Fe concentration. We note that Au carried negligible magnetic moment. The local moment of Fe actually increases with decreasing Fe concentration. This was also observed in earlier studies of Fe overlayers on Au. It can be attributed to the fact that in the lower Fe concentration alloys, there is a large probability of configuration in which we have small Fe clusters surrounded by non-magnetic Au host. The magnetic moment of small free clusters is much larger than bulk Fe. Immersed clusters have densities broadened as compared to free clusters because of hybridization with the environment.

However, since Fe and Au bands do not hybridize much, in these concentrations we observe local moments slightly larger than the higher concentration alloys.

The behaviour of Au and Co bands in AuCo and Au and Ni bands in AuNi are rather similar to the AuFe alloys. The spin-splitting of the Co bands is smaller than that of Fe, and that of Ni bands if even smaller, otherwise the qualitative behaviour is quite similar. Figure 2(b) shows the monotonic increase of the Fermi energy with Co concentration. The bowing is concave for AuCo as compared to AuFe, while that for AuNi is almost linear. This is sensitively dependent of the shapes of the density of states. Similarly, the alloying energy increases with increasing Co or Ni concentration, indicating greater stability of the higher Co or Ni concentration alloys.

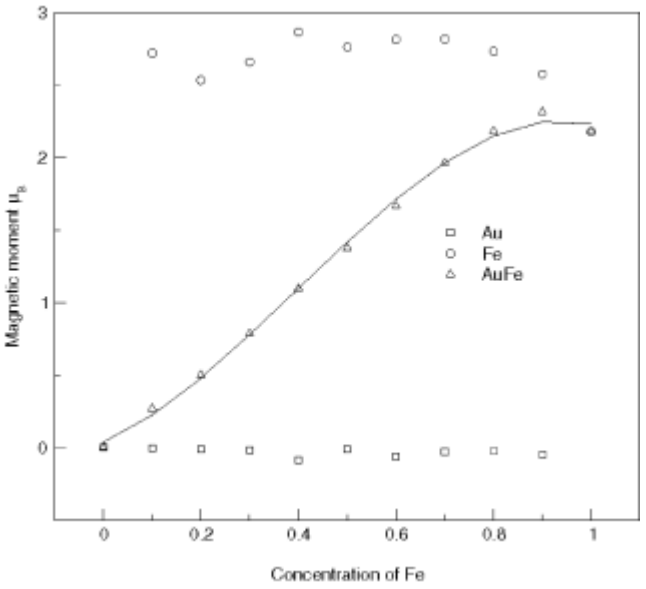

Figure 3a. Local and total magnetic moment for AuFe for different concentrations.

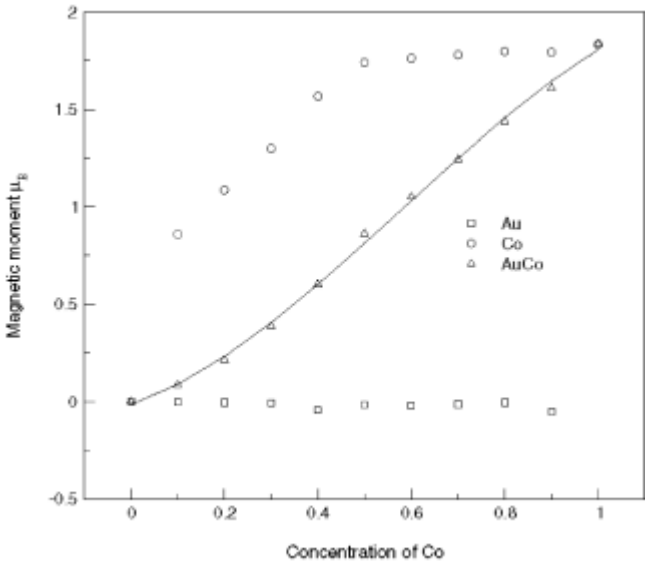

Figure 3b. Local and total magnetic moment for AuCo for different concentrations.

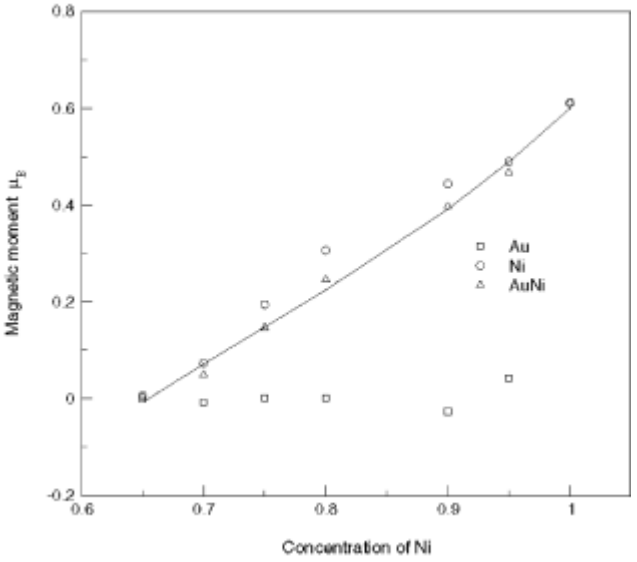

Figure 3c. Local and total magnetic moment for AuNi for different concentrations.

Figure 3(b) shows the behaviour of the local magnetic moments on Co and Au as well as the total magnetic moment of the alloy (per atom) as functions of Co concentration. Here the behaviour of the local moments on Co are quite different from those on Fe in AuFe. The local magnetic moment on Co is smaller than that on Fe. It appears that Co can sustain local magnetic moment upto 50% Co concentration. Below this, when Co atoms get progressively surrounded with more Au atoms, the Co atom rapidly begins to lose its local moment as the concentration of Au increases.

Figure 3(c) shows the behaviour of the local magnetic moments on Ni and Au as well as the total magnetic moment of the alloy (per atom) as functions of Ni concentration. We note that not only is the moment on Ni much smaller than those on Fe and Co, the local moment is extremely fragile. Ni begins to lose its magnetic moment as soon as it is alloyed with Au, and loses all its moment at 50% Ni concentrations. This means that of the twelve nearest neighbours of a Ni atom in the *fcc* alloy, it requires statistically seven or more of them to be Ni, otherwise the central Ni loses its magnetic moment. This fragility of Ni moment has been commented on earlier, and should be taken into account if we are setting up a Heisenberg like effective model for Ni alloys. This leads to a concentration dependent effective exchange, $J_{ij}(x)$.

4. Conclusion

We have proposed a methodology for the study of how electronic and magnetic properties change on alloying a

transition metal with a noble metal. When we wish to design a material with specific properties, this systematic study of behaviour with alloying will be essential if we wish to predict how to design such a material.

Acknowledgement

We thank the International Centre for Theoretical Physics, Trieste, for the financial help through its Network programme.

References

Andersen O K and Jepsen O 1984 *Phys. Rev. Lett.* **53** 2571

Biswas P, Sanyal B, Saha-Dasgupta T, Mookerjee A, Ahmad A, Huda A, Chaudhury N and Haldar A 1998 *J. Phys. Condens. Matter* **11** 1833

Blügel S 1997 in *Lecture notes, Workshop on electronic structure of surfaces* (Trieste: ICTP)

Dasgupta I, Saha T and Mookerjee A 1993 *Phys. Rev.* **B51** 17724

Dasgupta I, Saha T and Mookerjee A 1996 *J. Phys. Condens. Matter* **8** 1979

Ghosh S, Das N and Mookerjee A 1997 *J. Phys. Condens. Matter* **9** 10701

Ghosh S, Das N and Mookerjee A 1999 *Int. J. Mod. Phys.* **B13** 723

Gonis A, Turchi P E A, Kudrnovský J, Drchal V and Turek I 1996 *J. Phys. Condens. Matter* **8** 7883

Mookerjee A and Prasad R 1993 *Phys. Rev.* **B48** 27724

Mookerjee A, Mehta A and Sanyal B 2000 in *Electronic structure of alloys, surfaces and clusters* (eds) A Mookerjee and D D Sarma (Gordon and Breach)

Saha T and Mookerjee A 1997 *J. Phys. Condens. Matter* **9** 2179

Saha T, Dasgupta I and Mookerjee A 1994 *J. Phys. Condens. Matter* **6** L245

Saha T, Dasgupta I and Mookerjee A 1996 *J. Phys. Condens. Matter* **8** 1979